Venus Volcanism: Initial Analysis from Magellan Data

JAMES W. HEAD, DONALD B. CAMPBELL, CHARLES ELACHI, JOHN E. GUEST, DAN P. MCKENZIE, R. STEPHEN SAUNDERS, GERALD G. SCHABER, GERALD SCHUBERT

Magellan images confirm that volcanism is widespread and has been fundamentally important in the formation and evolution of the crust of Venus. High-resolution imaging data reveal evidence for intrusion (dike formation and cryptodomes) and extrusion (a wide range of lava flows). Also observed are thousands of small shield volcanoes, larger edifices up to several hundred kilometers in diameter, massive outpourings of lavas, and local pyroclastic deposits. Although most features are consistent with basaltic compositions, a number of large pancake-like domes are morphologically similar to rhyolite-dacite domes on Earth. Flows and sinuous channels with lengths of many hundreds of kilometers suggest that extremely high effusion rates or very fluid magmas (perhaps komatiites) may be present. Volcanism is evident in various tectonic settings (coronae, linear extensional and compressional zones, mountain belts, upland rises, highland plateaus, and tesserae). Volcanic resurfacing rates appear to be low (less than 2 km^3/yr) but the significance of dike formation and intrusions, and the mode of crustal formation and loss remain to be established.

VOLCANO-LIKE FEATURES ON VENUS were first detected in images from Earth-based radio telescopes and in Pioneer Venus topography (*1–4*). Higher resolution Earth-based and Venera images showed widespread plains volcanism and abundant volcanic centers and edifices of a variety of sizes and associations (*5–9*). These data confirmed that volcanism has been an important process forming and modifying the surface of Venus on a regional scale. Geochemical data from five Venera landers indicated that the surface at all but one landing site is similar in major element composition to that of tholeiitic and alkali basalts (*10–11*). Gamma-ray spectrometer data from the Venera 8 site, however, was interpreted to indicate an intermediate to silicic composition (*12–14*). Theoretical studies of the ascent and eruption of magma on Venus (*15*) assessed the influence of the high surface atmospheric pressure (4 to 10 MPa) and surface temperatures (650 to 750 K) on eruption conditions. Other analyses explored the derivation of magmas and melting of crustal materials in different petrogenetic environments (*16–18*).

The resolution of pre-Magellan image data, however, was insufficient to identify the detailed characteristics of many of the volcanic features and to assess the global distribution of volcanism and its tectonic relations. The Magellan mission, with its global high-resolution imaging (*19*), altimetry, surface properties (*20*), and gravity measurements, is designed to investigate many fundamental volcanological questions. In this report we discuss initial image and altimetry data for an area covering about 15% of the surface and analyze emplacement and eruption conditions and the geological and tectonic associations of volcanism.

Modes of occurrence. Magellan data confirm that volcanic edifices on Venus have a wide range of sizes and a diversity of shapes (Fig. 1). The most common edifice is the small dome or shield, which generally has a circular planimetric outline, a height of less than 100 to 200 m, and diameters of 2 to 8 km, but up to ~20 km. Approximately 22,000 were mapped in the 25% of the surface observed by Venera 15 and 16 (*8, 21*). These features were interpreted to be analogous to seamounts or other small shield volcanoes in Hawaii and Iceland (*8, 22*), but resolution was insufficient to determine their detailed surface morphology, summit characteristics, and structural associations.

Magellan data reveal these characteristics in detail. Four basic types of small edifices have been observed: (i) shield-shaped (uniformly low slopes and broad rounded summits; Fig. 1, C and D), (ii) flat-topped or table-like (steeper flank slopes and flat summits; Fig. 1, A and E), (iii) dome-shaped (steep, nonuniform slopes and broad summits; Fig. 1, G and H), and (iv) cone-shaped (Fig. 1F). The most abundant is the shield type, which typically has a single summit pit averaging ~700 m in diameter. Small edifices occur both as isolated features in plains or in clusters. In Guinevere Planitia (35°N, 330°; Fig. 2), a large (several thousand kilometers squared) area of dark plains partially superposed on a distinctive structural fabric of small parallel graben, a cluster of 55 edifices from 1.3 to 6.5 km in diameter are observed. Shield shapes comprise almost 90% of the population; the remaining edifices are mostly flat-topped. Over 90% of the shields have single summit craters or pits, but some double pits or summit domes are observed.

Small shield volcanoes on Earth commonly have summit craters that are linked to central lava conduits and summit lava lakes, which occasionally overflow. The resulting lava flows build up the edifice and drainback of lava into the conduit forms the pit [for example, as observed at Mauna Ulu, Hawaii (*23*)]. Few such discrete flows have been observed on Venus shields, perhaps because

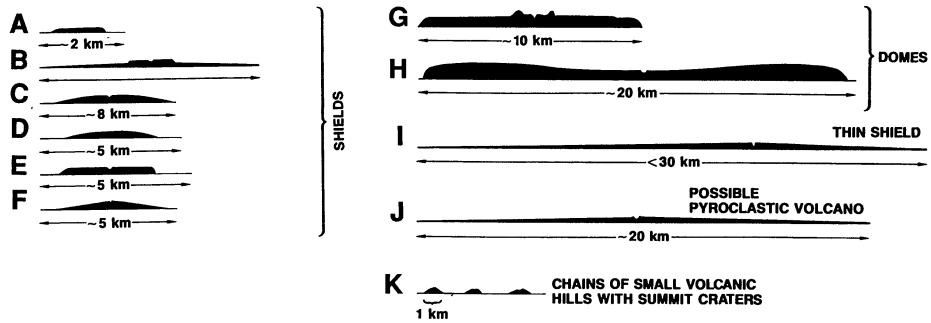

Fig. 1. Diagrammatic cross sections of some typical volcanic edifices in the plains of Venus. Shields most commonly range in diameter from 2 to 8 km and may be slightly flat-topped (**A**), have a superposed flat summit area (**B**), be convex upward with (**C**) or without (**D**) a summit pit, mesa-like (**E**), or like a low cone (**F**). Larger domes in the 10- to 25-km-diameter range have narrow steep sides with summit structures (**G**) or with a depressed interior (**H**). Some widespread radar dark deposits with summit pits appear to be low shields. Less common are craters surrounded by extensive dark annuli which appear to be small edifices surrounded by pyroclastic mantles (**I**). Fractures are observed that have chains of small volcanic hills with summit craters (**K**). M. Bulmer assisted in compilation.

J. W. Head, Department of Geological Sciences, Brown University, Providence, Rhode Island 02912.
D. B. Campbell, Department of Astronomy, Cornell University, Ithaca, NY 14853.
C. Elachi, Jet Propulsion Laboratory, 4800 Oak Grove Drive, Pasadena, CA 91109.
J. E. Guest, University of London Observatory, University College London, Mill Hill Park, London, England NW72QS.
D. P. McKenzie, Bullard Laboratories, Department of Earth Sciences, Cambridge University, Cambridge, England CB30EZ.
R. S. Saunders, Jet Propulsion Laboratory, 4800 Oak Grove Drive, Pasadena, CA 91109.
G. G. Schaber, U.S. Geological Survey, 2255 North Gemini Drive, Flagstaff, AZ 86001.
G. Schubert, Department of Earth and Space Sciences, Institute of Geophysics and Planetary Physics, University of California at Los Angeles, Los Angeles, CA 90024.

of resolution or lack of radar contrast, but the shields are the most likely source of the local intershield dark plains of Guinevere Planitia (Fig. 2). Most flows associated with these types of shields on Earth have relatively low volumes and low effusion rates (*23*). The small volume of Venus shields and associated lavas, <1% of the total crustal volume, suggest that individual shields have not contributed significantly to resurfacing (*8, 22*). However, continued formation of these features and their burial and coalescence (*24*) could lead to crustal thickening over long periods of time.

A group of irregularly shaped pits up to nearly 3 km in diameter are seen in the plains west of Alpha (Fig. 3). Channels about 1 km wide narrow away from the pits, particularly to the east, and extend downslope for 10 km or more. Although considerably larger, these features are similar in morphology to terrestrial lava channels on small shields and cones (*23*). They are comparable in scale and morphology to some sinuous rilles on the moon that may have formed by thermal erosion (*25, 26*), drainage, or the collapse of an extremely large lava tube (*27*).

There is a strong association of shields with regional structural patterns. Many summit pits are located (but not elongated) along graben, and graben also commonly cut the summit pit area. These relations suggest that some small graben represent the surface manifestation of dikes that supplied magma to the edifice. The most likely sources for the shield clusters are local thermal anomalies, whereas other edifices could form anywhere along regionally propagating dikes.

Larger edifices and volcanic centers have more complex summit structures and are less numerous. Slyuta and Kreslavsky (*28*) mapped about 800 intermediate-sized edifices (20 to 100 km) in the Venera 15–16 area. A shield about 50 km in diameter in northern Lada Terra (42.6°S, 27.9°) (Fig. 4) shows a central caldera-like structure about 12 km in diameter surrounded by an asymmetrical annulus of flows 1 to 2 km wide and extending for 15 to 40 km. To the north and northeast, an apron of flows 4 to 6 km wide largely underlies the annulus and extends up to an additional 60 km.

About 50 edifices with diameters of 100 to 350 km were mapped in the 45% of the surface covered by Venera and Arecibo data (*7, 9, 29–31*). One such example is Sif Mons, a 300-km-diameter peak rising 1.7 km above the broad 2-km rise of Western Eistla Regio (Fig. 5). Magellan data confirm that Sif Mons is a volcanic structure (*6, 9, 32, 33*) and reveal significant new details and age relations. The broad rise of Western Eistla Regio (Fig. 5, A and B) is characterized by a wide variety of volcanic plains (Fig. 5, C and D). About 400 km SSE of Sif, a concentration of small shields and associated flows embays these plains. A series of generally radial fractures and troughs 2 to 6 km apart are well developed on units in the northwest quadrant of Sif Mons. Near the volcano, fractures are heavily concentrated along a NW trend on both sides in a zone, ~100 to 150 km wide (Fig. 5D).

Subsequent to the formation of the various fractures, lavas originating from vents in and near Sif Mons were emplaced. For example, a radar-bright flow unit 15 to 30 km wide and 250 to 300 km in length emerged from a vent on the northern flank of Sif and flowed downslope to the north, embaying and flowing around low shields in the plains (Fig. 5, C to E). A similar unit (Fig. 5, D and F) appears to have flowed over 400 km from a vent below the summit of Sif toward the north until it reached a topographic low that caused it to turn and flow westward (Fig. 5, C and D). The ends of some of these long flow units (digitate plains) show increased emissivity values, perhaps because of a change in surface roughness with distance (*20*). On the basis of their extreme length, they may have been characterized by extremely high effusion rates or by very low viscosities (*34*).

Although these flows extend for great distances (Fig. 5H), they are of limited

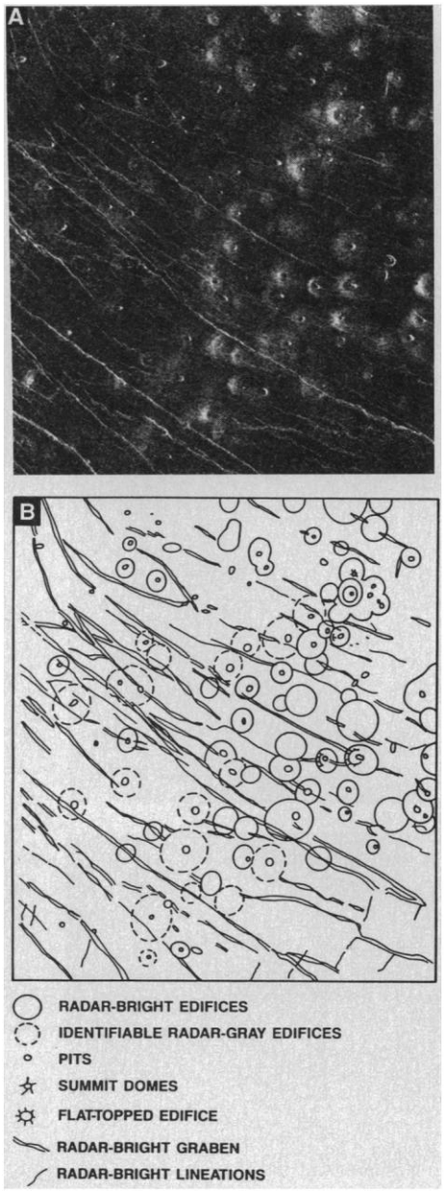

Fig. 2. Cluster of volcanic shields in Guinevere Planitia (35°N, 330°). (**A**) Magellan image of the region. Width of image is about 120 km. North is at top in this and all other figures except where noted. (**B**) Sketch map [by J. Aubele and E. Slyuta].

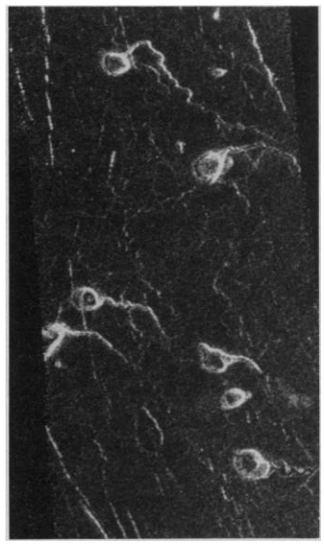

Fig. 3. Volcanic craters and associated sinuous channels in volcanic plains west of Alpha. Width of image is 24 km.

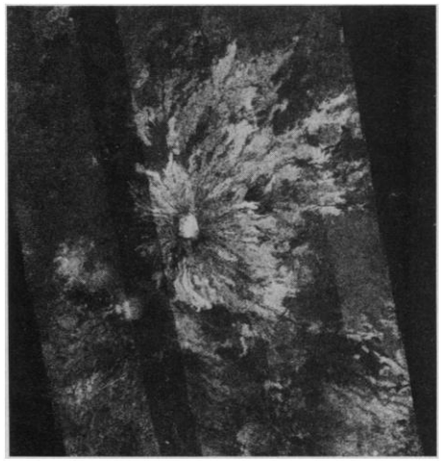

Fig. 4. Intermediate-sized shield volcano about 50 km in diameter in northern Lada Terra (42.6°S, 27.9°). Width of image is about 100 km.

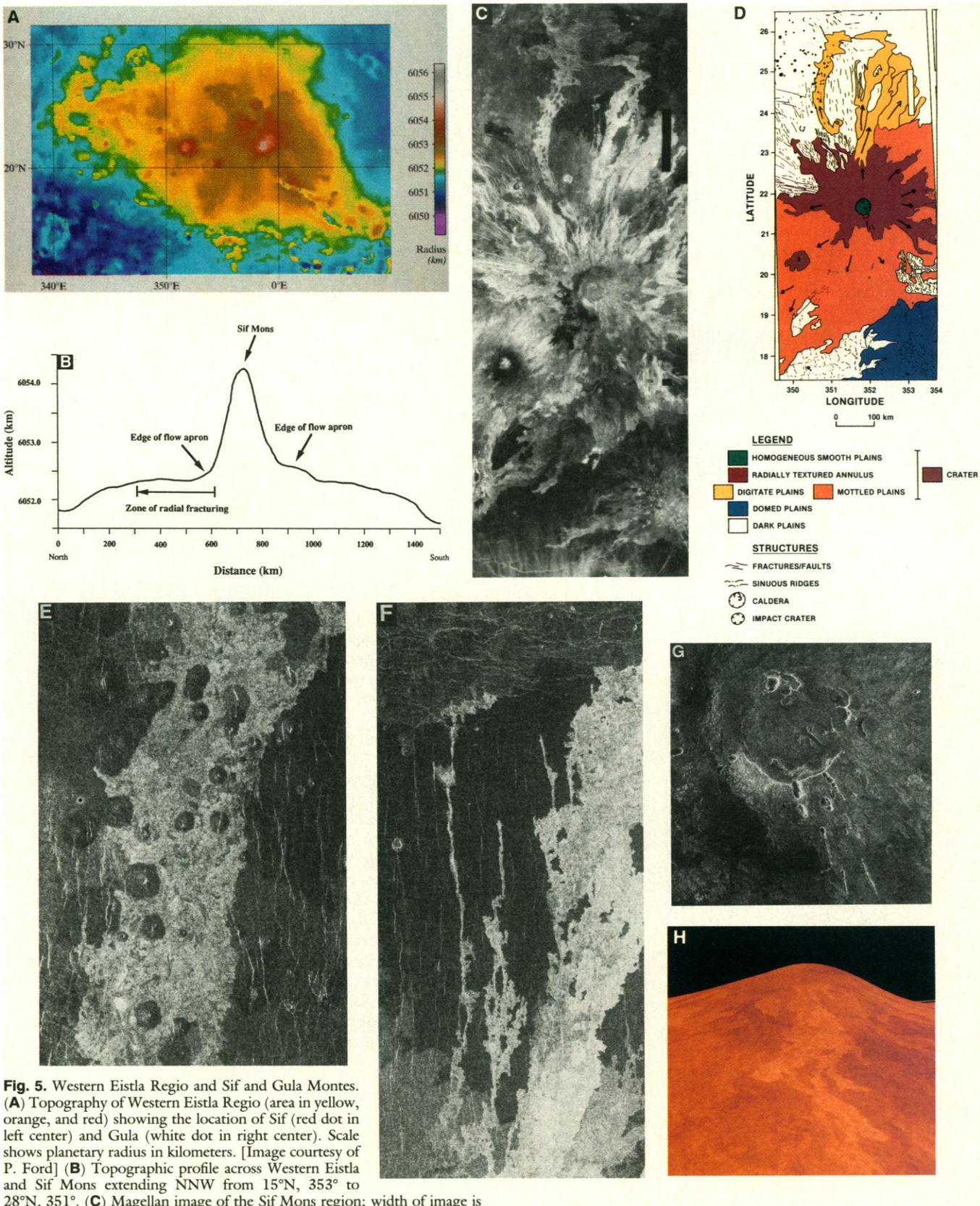

Fig. 5. Western Eistla Regio and Sif and Gula Montes. (**A**) Topography of Western Eistla Regio (area in yellow, orange, and red) showing the location of Sif (red dot in left center) and Gula (white dot in right center). Scale shows planetary radius in kilometers. [Image courtesy of P. Ford] (**B**) Topographic profile across Western Eistla and Sif Mons extending NNW from 15°N, 353° to 28°N, 351°. (**C**) Magellan image of the Sif Mons region; width of image is 450 km. (**D**) Sketch map of the Sif Mons region [by D. Senske]. (**E**) Flow unit of digitate plains flowing northward and embaying small shields in the regional dark plains. Note that fractures postdate plains and domes, but predate flow unit. Width of image is 55 km. (**F**) Flow unit of digitate plains flowing northward and being locally diverted into small graben developed in the background plains. Width of image is 65 km. (**G**) Summit region of Sif Mons showing small pit craters and smooth plains. Width of image is 85 km. (**H**) Perspective view of Sif Mons using Magellan images superposed on topography. Color is simulated. View is from the northeast. Bright flows are ~3 to 8 km in width [by E. De Jong, J. Hall, and M. McAuley].

extent compared to the overall dimensions of the Eistla rise (2000 km by 2800 km; Fig. 5, A and B). They appear to be a relatively thin veneer of material.

A blanket of multiple flows and flow units having variable radar backscatter (mottled plains) extends up to 300 to 500 km east and south from the summit region. Most of these units appear to have their sources in the summit region; some units originated from local flank eruptions. An apron or annulus generally 100 to 150 km in width and composed of radially textured flow units surrounds the summit area and makes up most of the summit region.

A caldera-like feature 40 to 50 km in diameter characterizes the summit of Sif Mons; relatively homogeneous smooth plains with locally high reflectivity values (*20*) (Fig. 5G) appear to fill the caldera to near the rim, perhaps overflowing in places. The caldera and SE part of the annulus contain numerous 3- to 10-km-diameter circular to elongate depressions and chains generally oriented NW-SE (Fig. 5D). These features are interpreted to represent smaller calderas and collapse pits associated with flank intrusions and eruptions. The NW-SE structural trend is also reflected in both the broad-scale topography of Western Eistla Regio (Fig. 5A) and the enhanced distribution of deposits surrounding Sif Mons to the NE and SW down the regional slopes.

The large size of the summit structure (Fig. 5G) suggests that it formed by large-scale evacuation of magma perhaps linked to intrusion along the NW-SE rift zone, or to one or more of the larger flows on the flanks (Fig. 5, C and D). The smaller 3- to 10-km-diameter craters are more comparable in size to the 4-km-diameter Kilauea caldera, Hawaii, and these appear to be formed by local collapse linked to the smaller-volume, near-summit flows.

These relations, and the association with a broad rise, suggest that a thermal plume or hot spot may have uplifted and fractured Western Eistla radially and locally along a NW trend. Voluminous melts associated with the plume head followed by numerous smaller eruptions as the plume evolved may have built the edifice. The age of activity at Sif is unknown. One impact crater is superposed on the edifice deposits (Fig. 5, C and D), and several other probable impact craters are in the vicinity.

Sachs Patera, an elliptical depression located to the south of Lakshmi Planum, shows a more complex structure than Sif Mons (Fig. 6). Sachs is characterized by a circular depression 40 km in diameter and 130 m deep and a 30-km-diameter arcuate region to the north. This nested structure suggests that two stages of collapse of a caldera may have occurred. A small arcuate region 7 km in diameter along the southwest rim of the depression may represent a third stage of caldera collapse. The walls of the caldera are composed of concentric scarps separated by distances of 2 to 5 km. Although radar-bright flow deposits extend for distances of 10 to 25 km from the northern rim of the caldera, there is little topographic evidence (other than a 120-m high on the NE rim) that the flow deposits are associated with a major constructional edifice. The morphology of this caldera suggests that it was formed by downsagging. Much of the evacuated magma may have been transported along dikes and erupted at fissures to the south, similar to the relation seen in many terrestrial calderas (*35*).

The largest caldera-like structure observed so far is Sacajawea Patera, a depression in Lakshmi Planum, Western Ishtar Terra, that is 200 by 300 km in diameter and 1 to 2 km deep (*36, 37*). The volume of the depression, $\sim 2 \times 10^4$ to 6×10^4 km^3, is considerably greater than volumes of typical terrestrial and martian calderas (*37*). Magellan data show that an annulus of volcanic plains (Spu) 120 by 215 km occurs in the depression surrounding mottled bright deposits (Spm) (Fig. 7, A to D). The elevation of the northern rim averages 600 m higher than the southern rim (Fig. 7E), and the patera floor is 0.4 to 1.7 km below the surrounding plains. Only a few radial flow features are observed (Fig. 7, A to C), and no shield edifice comparable to Sif Mons is observed in either image or altimetry data. A distinctive single ridge or scarp as on collapse caldera margins on Earth is also not evident. Instead, the margin is a wide belt of concentric faults, many of which are graben 4 to 100 km in length, 1 to 2 km in width, and spaced several kilometers apart. Farther out, the fractures become less distinct, particularly to the north and south, and shorter (3 to 10 km). Numerous lineaments cross cut the fractures to the west and east. Zlata, a 6-km impact crater NW of Sacajawea, apparently postdates graben formation.

Extending from the SE boundary of Sacajawea is a system of linear features (Fig. 7D) that were interpreted as graben from the Venera data (*36, 37*) but appear more sinuous and ridge-like in the Magellan images. A shield volcano 12 km in diameter with a prominent central pit lies along the trend of one of these linear structures. This association and the presence of mottled, lobate flows (Fig. 7C) suggests that the lineations may represent a flanking rift zone along which the lateral injection and eruption of magma has occurred. A flow complex on the SW flank of Sacajawea was observed in the Venera data (*37*), and flow units embaying the concentric fractures seen in the Magellan data suggest that subsidence and extrusion of lava were taking place simultaneously.

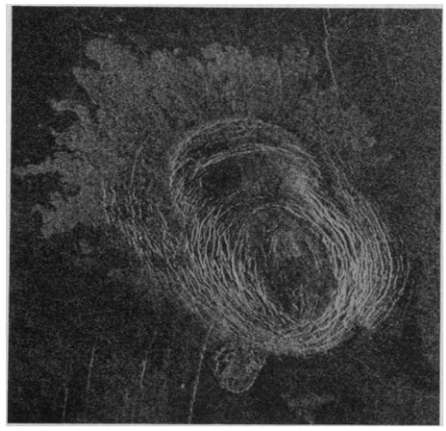

Fig. 6. Sachs Patera located in Sedna Planitia.

This analysis suggests the following history for the region. Magma rising from depth reached neutral buoyancy in the upper part of the crust in eastern Lakshmi Planum (*38*) and created a large magma reservoir. Magma was predominantly intruded laterally along dikes. Continued lateral eruption partially emptied the magma reservoir and resulted in broad sagging and downwarping of the overlying rocks and formation of the annulus of graben, the nature and spacing of which suggest that they may represent brittle deformation of a crustal layer a few kilometers thick. This distinctive structure may result from the combination of elevated upper crustal temperatures above a large magma chamber and the high surface temperatures typical of Venus. The large caldera volume suggests that the load of the relatively dense solidifying magma reservoir contributed to the broad-scale subsidence (*37*) producing the sag-caldera. Concurrently with the downwarping, magma injected distally along dikes occasionally erupted to flood the outer edge of the annulus of graben. In the latest stages of subsidence, lava flooded the caldera, perhaps creating a lava lake several hundred meters deep, which subsequently drained and was deformed. The youngest lavas appear to have been emplaced on the crater floor in a topographic annulus. Thus, both Sacajawea and Sachs paterae, with their annulae of graben and lack of significant edifice deposits, represent a distinctive type of sag-caldera unlike typical calderas seen on basaltic shields such as Hawaii and Sif Mons. In addition, Sacajawea Patera is distinct in terms of its size and location in the highlands. Comparison to Colette, about 600 km west of Sacajawea and not yet mapped by Magellan, will shed

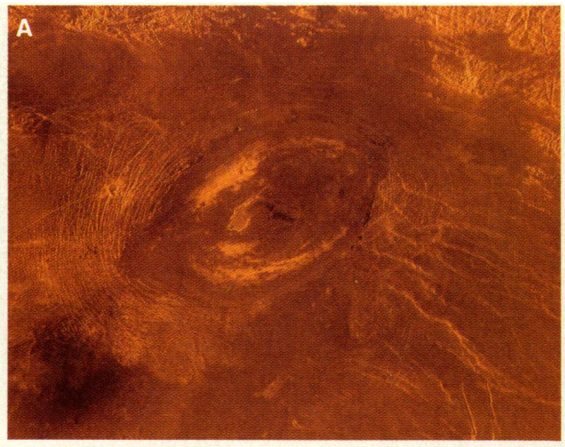

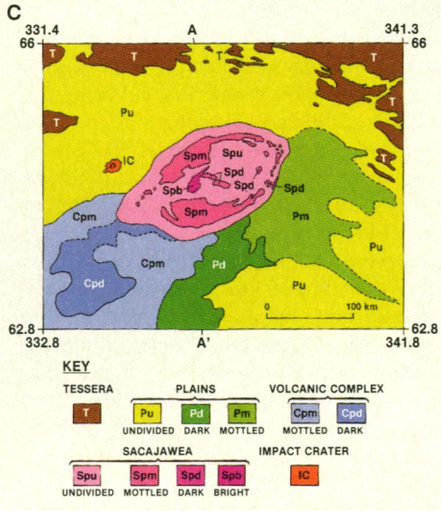

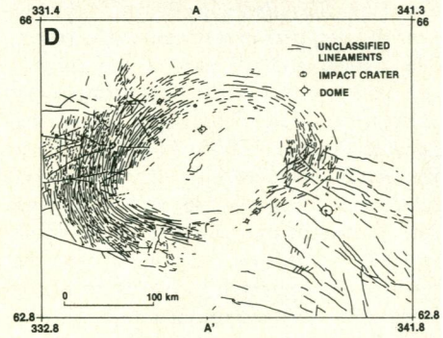

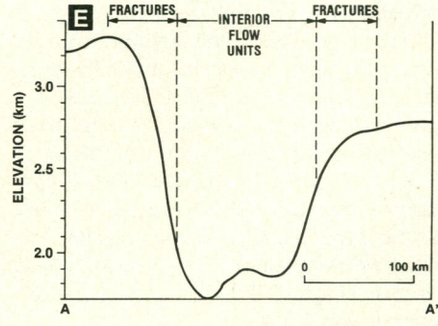

Fig. 7. Sacajawea Patera, Lakshmi Planum, Western Ishtar Terra. (**A**) Magellan image of Sacajawea Patera. Width of image is about 420 km. North is at top. Color is simulated. (**B**) Enlargement of the area at the SW edge of Sacajawea showing the interior plains and details of the graben. North is to left. (**C**) Geologic sketch map. (**D**) Structural sketch map. (**E**) Topographic profile showing the relations of topography, units and structure. Location of profile is shown in (**D**). [Maps by K. Roberts]

more light on the history of this region.

The high surface atmospheric pressure of Venus should act to inhibit the exsolution of volatiles from ascending magmas that leads to pyroclastic activity unless the volatile content exceeds about 4% by weight (*15*). Thus, identification of pyroclastic deposits and mantles may provide evidence for eruption of magmas with enhanced volatiles. One possible site (Fig. 8) is in Guinevere Planitia nearly 0.5 km below the Venus datum where atmospheric pressure is between 9.0 and 9.5 MPa. Here, shields with 1-km-wide summit craters are associated with a radar-dark unit that appears to mantle the reticulate patterned plains. Thinning of the mantle away from the crater may be interpreted as the result of explosive volcanism and deposition of tephra. If this is correct, the extensive nature of the deposits (20 km diameter or more) suggests a plinian style of eruption. On Venus, coarse tephra should fall close to the vent (*15*) and distal deposits should be fine-grained material carried convectively in the plume.

Radar-bright pie-shaped areas to the south of the craters appear to be regions that have been stripped of the fine-grained mantle. Removal may have been by eddies in prevailing winds, induced by the presence of the crater and shield. Local darkening of the margins of the bright areas suggests that material may be thicker at the edges of the eroded zone than elsewhere. The penetration characteristics of the relatively long wavelength of the radar (12.6 cm) (*39*) suggest that the minimum thicknesses for the mantle are 2.5 to 6 m.

Relatively steep-sided domes are also seen that are morphologically comparable to many dacite-rhyolite domes on Earth. The most impressive is a series of seven steep-sided volcanic domes located east of the highland Alpha Regio (30°S, 11° to 13°) (Fig. 9A). The domes are all about 25 km in diameter and have heights of 100 to 600 m; their volumes are thus 50 to 250 km^3, larger than volumes of most (but not all) rhyolite-dacite flows and domes on Earth, which are typically <1 km^3 (*40*). The two eastern domes have sharp contacts with the surrounding plains and well-defined fracture patterns, radial cracks on the outer steep slopes, an annulus of concentric ridges and cracks on the outer edge of the flat top, and an inner network of radial and concentric cracks (Fig. 9B). Similar terrestrial domes, formed by relatively high effective viscosity magmas (*41*), are characterized by (i) intrusion of magma from a central conduit under a brittle, cooled carapace causing expansion and growth of the dome (endogenous activity); and (ii) breakthrough of flows or small extrusions, and explosive activity (exogenous activity) (*42–45*). We interpret the Venus domes to be formed by similar processes; the central pits may represent the final degassing of the magma, possibly explosively. The three western domes appear to have the most complex history, and at least two have associated summit and flank cones and possible flows.

The large volume of the domes may be due to the higher surface temperature on Venus, which might permit magma to extrude more efficiently and to cool more slowly and thus travel for greater distances than similar magmas on Earth. The distinctive circular planform of the domes may be a result of the level substrate.

Three similar steep-sided domes 8 to 15 km in diameter are located in northern Lavinia Planitia (30°S, 338°) and surrounded by abundant lineaments and fractures (Fig. 10). The two northern structures appear to have summit cones and possible short, stubby flows. The southern dome shows little evidence for flows or cones and probably grew mostly by endogenous activity similar to the domes just east of Alpha (Fig. 9). On Earth, such domes (Figs. 9 and 10) form in a wide variety of geological and

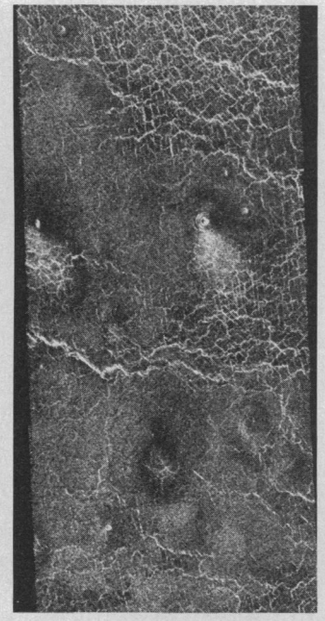

Fig. 8. Regional deposits of possible pyroclastic origin mantle highly fractured plains in southern Guinevere Planitia. Width of image is 40 km.

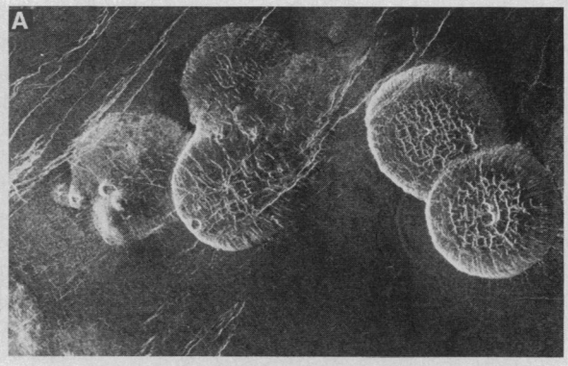

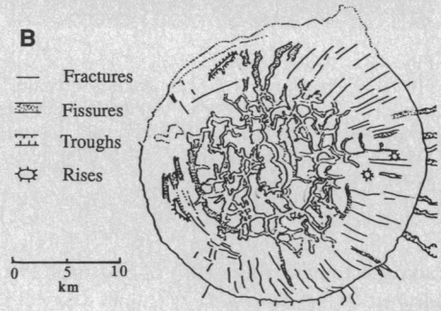

Fig. 9. Domes located southeast of Alpha Regio (30°S, 11° to 13°). (**A**) Magellan image of domes, each about 25 km in diameter. The westernmost five of the seven domes are shown. The arcuate line in plains west of the easternmost dome is a radar artifact. North is at top. (**B**) Sketch map showing major morphologic features of southeasternmost of these domes [by B. Pavri and B. Klose].

petrogenetic environments (*46, 47*) including in association with continental volcanism and large calderas (for example, Long Valley, California, and Valles, New Mexico). Some of these domes may be transitional with intrusive cryptodomes.

A steep-sided truncated conical volcanic structure about 8 km in diameter and hundreds of meters high (Fig. 11) is located several tens of kilometers north of the domes in Fig. 10. The contact of the volcano with the surrounding plains is sharp, and the large summit pit, almost 3 km in diameter, is larger than summit pits observed on other steep-sided domes and may be evidence of explosive eruptions or subsidence and collapse of the summit. Radial grooves occur on the slopes, and the general morphology is similar to that of tholi seen on Mars, although tholi are much larger. These characteristics suggest that the magma involved was viscous, as would be the case for intermediate to acidic compositions.

Additional evidence for silicic compositions comes from the gamma-spectrometric measurements of Venera 8, which showed that the material at the landing site (10°S; 335°) contains concentrations of K (4.0 ± 1.2% by weight), U (2.2 ± 0.7 ppm), and Th (6.5 ± 0.2 ppm) that are higher than typical in terrestrial basalts (*12*). Later landers at other sites reported primarily basaltic compositions, however (*10, 11*). The materials at the Venera 8 site have been variously characterized as silicic calc-alkaline (possibly granite), intermediate sub-alkaline (shoshonitic), syenitic, intermediate alkaline (nepheline syenite), and alkaline basalt. Recent analyses (*14*) show that the Venera 8 material falls off the normal calc-alkaline magmatic trend and is geochemically close to the quartz monzonite–quartz syenite group of terrestrial igneous rocks, which make up a significant part of Earth's continental crust. On the basis of these data, Nikolaeva (*14*) proposed that such material may lie beneath the apparently widespread basaltic plains.

Magellan images (Fig. 12) show that Venera 8 landed (about 1° uncertainty in the location of the landing site) in a region of mottled plains, a pancake-like dome 22 by 25 km in diameter, and a complex of radar-bright and -dark flow units related to NW trending fractures in the plains and interpreted to be basaltic flows. The pancake-like dome is surrounded by a concentric fracture pattern extending out some 10 to 15 km and has an outer annulus ~5 to 6 km wide with steep slopes and an inner shallow depression 10 by 12 km across that contains several shallow rimless pits. The similarity of this pancake-like dome to rhyolite, dacite, and andesite domes on Earth and to the steep-sided domes seen in Figs. 9 and 10 suggests that the rocks measured by Venera 8 may be related to the pancake-like structures (*47a*).

Styles of emplacement and eruption conditions. In terrestrial volcanic environments, the majority of magma is intruded as dikes and other subsurface bodies and only approximately 10 to 20% (depending largely on environment and density factors) is extruded to form flows and edifices (*48*). The ratio of intrusion to extrusion is unknown for Venus but several factors argue that it may be lower than for Earth (*15*) including: (i) the depth to a specific magma compaction state is slightly less for Venus (*38*), (ii) inhibition of vesiculation by high atmospheric pressure on Venus acts to decrease melt/rock density differences (*15*), and (iii) high-density crust is more abundant on Venus. The likelihood that magmas reach neutral buoyancy at shallower levels in the crust on Venus than on Earth (*38*) may

Fig. 10. Three steep-sided, generally flat-topped domes 8 to 15 km in diameter located in northern Lavinia Planitia (30°S, 338°).

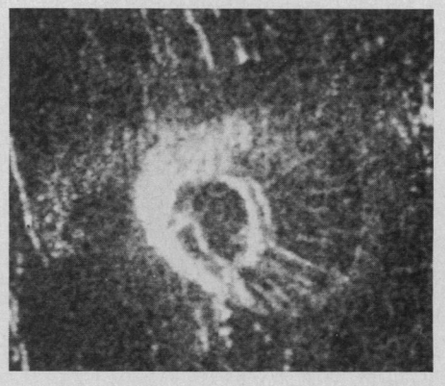

Fig. 11. Truncated cone about 8 km in diameter and located a few tens of kilometers north of the domes in Fig. 10.

Fig. 12. Magellan image of the Venera 8 site (10°S, 335°E) showing the occurrence of basaltic plains and steep-sided domes within the area of uncertainty in location of the landing site (about 100 km radius around X). Width of image is about 200 km. (*82*).

account for the abundance of fractures and graben associated with volcanic deposits; such fractures (Figs. 2, 7, 10, and 13) are evidence of abundant dikes (*49*). In the 50-km-diameter volcanic feature in Fig. 13, fractures are generally radial near the structure (in response to stresses associated with the magma reservoir), but are oriented generally N-S at greater distances [where they may be controlled by regional N-S compression (*50*)].

Other types of shallow intrusions are also evident. The easternmost of three relatively flat-topped domes in the dark fractured plains of Sedna Planitia (36°N, 330°) (Fig. 14) has slopes in excess of 10°. The top of the dome is fractured in a star-like pattern, and some fractures widen to grooves up to 500 m wide, a few of which extend down slope. This pattern is somewhat similar to that in the domes in Figs. 9 and 10, but the different crest, marginal, and flank deposits and structures suggest that it formed by up-doming and fracturing of preexisting plains units, as for laccoliths and cryptodomes on Earth.

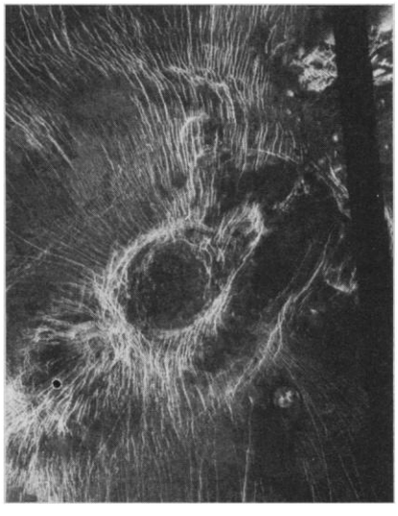

Fig. 13. Magellan image of circular structure about 50 km wide located 1500 km NW of Alpha Regio (16°S, 352°E). The structure is surrounded by a radiating fan of linear features similar to dike swarms in terrestrial environments.

The Magellan data show that fissure-related effusive eruptions have been common on Venus. One such area is in southern Guinevere Planitia (4.6°N, 331.8°E) where several radar-dark lava flows are seen (Fig. 15). In this and other examples, the radar brightness varies both within and among flow units, most likely because of variations in surface roughness (*6, 51*) at scales near the radar wavelength (12.6 cm), although variations in the dielectric properties of the surface material may contribute (*20*).

Flows have a wide range of morphologies. For example, the northern slope of the shield volcano at the source of Mylitta Fluctus (Fig. 16) displays a series of radar-bright flows averaging about 5 km in width and characterized by central channels and levees. Flows that extend beyond the base of the volcano are broader and have a diversity of features including braided channels, levees, breakouts, and textural changes between and within flows, and evidence for both tube-fed and sheet flows. Such structures are important in assessing eruption conditions, flow characteristics, and eruption rates (*15, 52*).

A number of sinuous channels have been discovered in the volcanic plains. As illustrated in southwest Guinevere Planitia (Fig. 17, A and B), these features commonly: (i) are about 0.5 to 1.5 km wide; (ii) have a constant width; (iii) lack associated flow lobes or lava flow deposits; and (iv) in some cases terminate in low-lying areas forming large plains deposits. The sinuous radar-dark rille-like feature in Fig. 17A is about 0.75 to 1.5 km in width. Details show what appear to be radar-bright levees and local breakouts. West of this area this rille winds its way across the plains and in between two ridges trending generally N-S, turning north and apparently emptying out into the low-lying plains to form the fan-shaped plains area. Its total length exceeds 1000 km.

These channels are similar to sinuous rilles on the moon that are interpreted to have formed when low-viscosity lava or lava emerging at high effusion rates becomes turbulent and thermally erodes and incises a channel into preexisting plains deposits (*25, 53, 54*). The high surface temperatures on Venus may enhance thermal erosion processes (*15*). Petrogenetic considerations suggest that fluid ferrobasalts and possibly even komatiites (high-temperature, Mg-rich lavas) may be common in certain environments on Venus (*16*), but further study is necessary to determine if they have produced these structures.

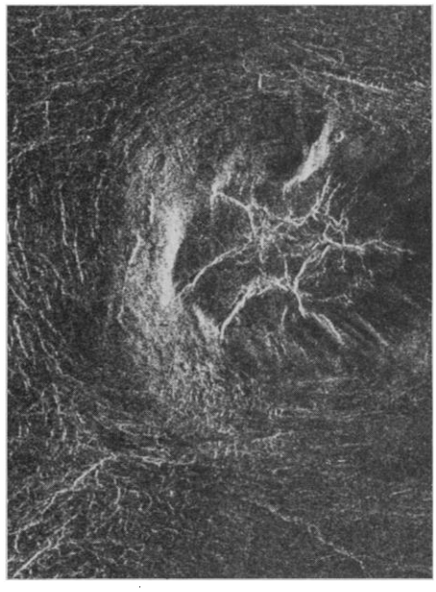

Fig. 14. Magellan image of a steep-sided, flat-topped dome measuring about 30 km at the base and 13 by 20 km at the crest located in Sedna Planitia (36°N, 330°). The dome differs from the morphology of extrusive domes in terms of surface patterns and contrast to surrounding materials, suggesting that it is intrusive rather than extrusive. On Earth such features form by shallow laccolithic intrusion and upbowing of the surface and are known as cryptodomes.

Large sinuous channels and complex channel patterns are also observed, for example in northern Lada Terra (50°S, 21°; Fig. 17C) where a massive outpouring of lava has created an extensive and spectacular drainage system that includes fluid-dynamically shaped islands, streamline structures, braiding, and abundant evidence of mechanical and thermal erosion. Although these features bear some morphological similarity to terrestrial and Martian channels of aqueous origin, their association with proximal volcanic source regions and their distinctive lobate flow morphology in the distal parts, together with the instability of liquid water on Venus at present, suggest that they originated from massive outpouring of fluid lavas.

Volcanic associations and environments. The associations of volcanic landforms and their physiographic and tectonic environments provide important information on the petrogenetic and mantle processes responsible for magmatism and the relation between tectonism and volcanism, both in terms of relative timing (for exam-

Fig. 15. Several radar-dark lava flows in southern Guinevere Planitia (4.6°N, 331.8°E) apparently emanating from a fissure, flowing west, and coalescing to form a larger deposit. Width of image is 35 km.

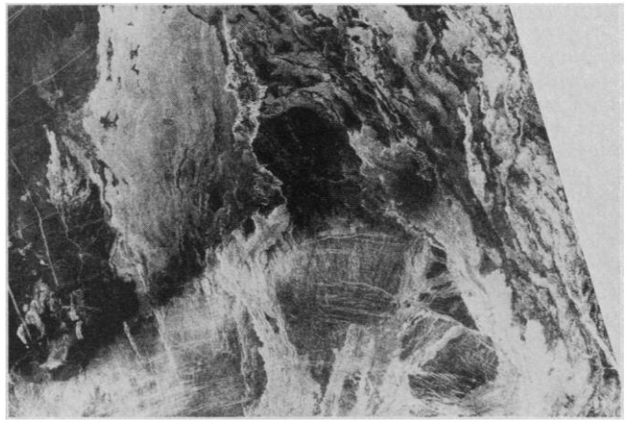

Fig. 16. Variations in lava flow morphology associated with the shield volcano at the source of Mylitta Fluctus (58°S, 353°). Width of image is about 315 km.

ple, vertical movements and associated melting) and genesis [for example, crustal thickening and melting, or stretching, upwelling, and pressure-release melting; (*16*)].

Regional plains deposits of probable volcanic origin form the vast majority of the surface observed in Guinevere, Sedna, and Lavinia Planitiae (*55*). Although lava flows and sources are abundant, as discussed above, it is not yet determined whether such volcanic activity was responsible for the formation of the crust as a whole (*56*), or whether it represents a veneer on other deposits produced in situ or elsewhere.

A wide variety of narrow linear deformation zones occurs on Venus including those of extensional (rift zones and some ridge belts), compressional (mountain belts and some ridge belts), and shear origin (*57*). Magellan data have revealed details of a volcanic source located along a linear deformation zone of extensional origin in northern Lada Terra (54°S, 354°) (Fig. 18). A family of lava flow units stream downslope into the adjacent Lavinia Planitia and form a lava complex [Mylitta Fluctus (*58*)] extending over 800 km N-S and 380 km E-W. Five broad flow units were outlined in Arecibo data (*59*). Magellan data show that most if not all of these lavas originated from a ~325-km-diameter, 700-m-high shield volcano located on the deformation zone (58.3°S, 351.5°) (Figs. 16 and 18, A and D). The shield edifice is defined by the margin of a relatively old, diffuse, bright deposit with a fine radial texture that is attributed to many closely spaced individual radial flow lobes. The source region is a central vent, ~20 by 40 km, that is surrounded by semiconcentric ridges and scarps; radial flow channels extend out to ~50 km to the NE and NW. Parts of the interior of the vent and immediate surrounds are characterized by deposits of extremely dark material. Some of the major flow units flowed directly north whereas others flowed east along the lineament belt before turning to the north (Fig. 16); an extensive unit of relatively homogeneous plains extends to the south and embays a 60-km impact crater (Fig. 18D). Three similar lava complexes at the eastern edge of Lavinia Planitia (51°S, 6°; 47°S, 5°; 45°S, 0°) were also mapped in the Arecibo data (*59*).

From the base of the edifice, the topography descends about 1 km over a distance of 500 km (a slope of about 0.11°) before flattening out in the last 75 to 185 km, where the flow units pond (Fig. 18B). The widths of individual flow units vary from 3 to 125 km. Individual flows within the major flow units are typically narrow (~3 km) and closely spaced near the source but widen substantially (to ~15 to 50 km) and are extremely uniform and homogeneous in surface texture north of ~56°S; this change may reflect the decrease in surface slope to the north. The oldest flow units appear to be those in the western half of the area (Fig. 16).

The brightest and longest flows in the

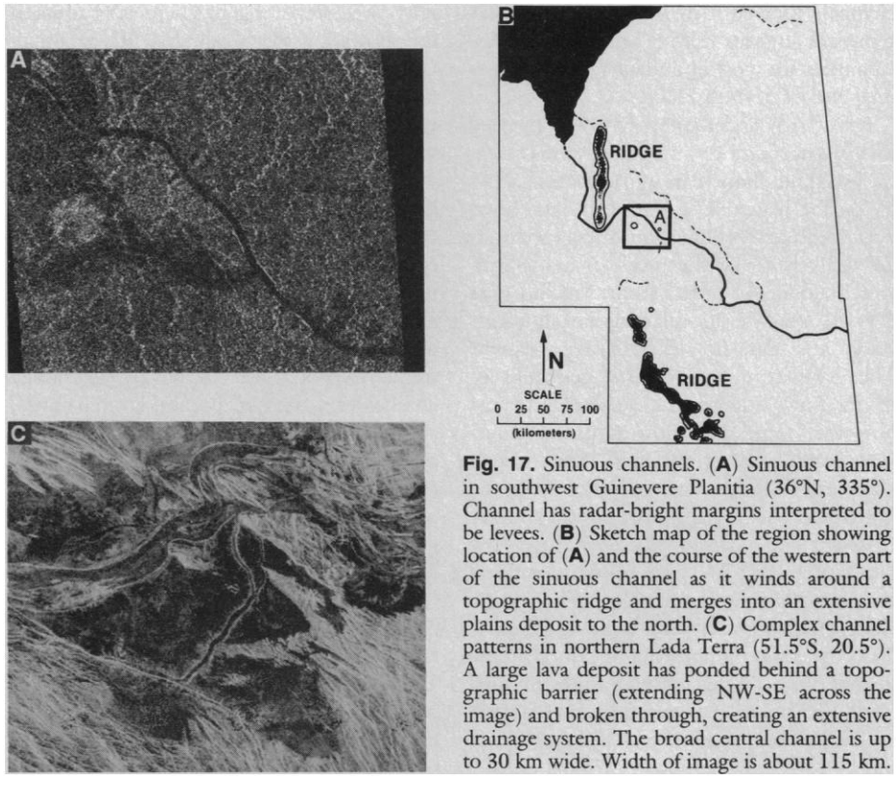

Fig. 17. Sinuous channels. (**A**) Sinuous channel in southwest Guinevere Planitia (36°N, 335°). Channel has radar-bright margins interpreted to be levees. (**B**) Sketch map of the region showing location of (**A**) and the course of the western part of the sinuous channel as it winds around a topographic ridge and merges into an extensive plains deposit to the north. (**C**) Complex channel patterns in northern Lada Terra (51.5°S, 20.5°). A large lava deposit has ponded behind a topographic barrier (extending NW-SE across the image) and broken through, creating an extensive drainage system. The broad central channel is up to 30 km wide. Width of image is about 115 km.

Fig. 18. Mylitta Fluctus (54°S, 354°) (*81*). (**A**) Arecibo image of southern Lavinia Planitia showing the massive outpouring of lavas downslope into Lavinia Planitia. Boxes indicate locations of Magellan images. (**B**) Magellan image showing the topographic control on flow emplacement in the low part of the basin adjacent to a ridge belt to the north. (**C**) Relatively homogeneous radar-bright lava flows in Lavinia Planitia. (**D**) Source region for many of the flows is a shield with elongate caldera located on the linear deformation zone.

eastern part of the field are distinctive for their uniform brightness and texture; few channels are observed in these flows (Fig. 18C). In contrast, many flows to the west appear to be mottled and have a bright margin and dark center. The dark center of some flows consists of channels, 0.7 to 3 km in width and up to 125 km long. Those channels that cut across several units may represent sinuous rilles (Fig. 17, A and B). Channels are most abundant near the proximal end of Mylitta Fluctus.

Kryuchkov and Basilevsky (*60*) suggested that bright rough flows represent the youngest (<200 million years ago) volcanic activity on the planet. The Magellan data, however, indicate that flow-brightness variations are unlikely to be the result of aging processes alone. As noted from Arecibo data (*59*), in detail the age relations among radar-bright and -dark flow deposits are complex. The flow complex consists generally of bright flows superposed on darker plains; however, some dark flow units are interleaved among the bright units (they are both older and younger than bright flows). In the northwest, lobate dark flows appear to have cross-cut and isolated older, brighter flow deposits (Fig. 18B). In addition, some flows change brightness gradually or abruptly along their course. Several factors, including dielectric constant and roughness, could influence flow brightness and these in turn could be linked to variations in magma rheology, composition, and thermal structure.

The extreme flow lengths observed in Mylitta Fluctus (300 to 800 km) suggest that the flows have low viscosity and low yield strength and are mafic lavas similar to some lunar mare basalts or terrestrial Archean komatiites (*28*). Implied effusion rates for these flows are high (about 10^5 m^3/s), and flow volumes (up to about 100 km^3) are comparable to volumes of some of the flows of the Columbia River Basalt Group (*61*), some of which exceed 1000 km^3. Some of the Mylitta Fluctus flows ponded in Lavinia might approach these values.

Coronae are 200- to 1000-km-diameter quasi-circular structures that are completely or partially surrounded by an annulus of concentric ridges and commonly have raised interior topography, a peripheral trough or moat, and numerous associated volcanic and tectonic landforms (*5, 62–64*). The interior of many coronae are covered by lava flows; and calderas, shields, domes, lava channels, and pits are observed there. Magellan images and topographic data over Quetzalpetlatl (68°S, 355°) in northern Lada Terra (*58*), one of the largest coronae on Venus, provide important data on the role of volcanism in the development of the corona.

Quetzalpetlatl rises more than 2 km above the surrounding plains and is covered by radar-bright and -dark lava flows (Fig. 19A). Only the annular ridges on the northwestern margin of the corona and some tectonic ridges and patches of high standing fractured terrain in the interior (perhaps the original updomed and radially fractured floor of the corona) are not covered by lavas. The source region for much of the volcanism is a depression located southeast of the corona center (*58*) that is 150 by 200 km and 400 m deep (Fig. 19B). Elliptical fractures coincide with the depression and are interpreted to be related to the formation of a caldera. The edifices within and to the east of the depression range in diameter from 4 to 15 km and have morphologies ranging from simple domical hills to conical and pancake-like structures. Many are oriented along the ENE trending axis of the inner caldera. Those that are near the rim are heavily influenced by the fracturing associated with the caldera; whereas those that are near the interior are more symmetrical. The domical hills are interpreted as volcanic shields similar to those seen in the plains (Figs. 1 and 2). Several of the edifices are complex structures that may be larger shields

(diameters of about 15 km) with summit calderas. One such edifice (right-center of Fig. 19B) has at least two summit depressions, a narrow (<500 m) channel similar to a sinuous rille extending SSE for at least 40 km, and two wide (3 km) troughs with rounded terminations on its eastern margin. North and slightly west of this edifice is a lower relief shield that is nearly cut in half by an irregular trough which is aligned with the elliptical fractures that surround the interior depression.

The presence of several steep-sided domes and shields in the interior (similar to those in Figs. 9 to 11) suggest that some viscous magmas may have been erupted. If so, the composition of the magma erupted from the volcanic center may have changed with time.

Some sources of flows occur outside the caldera and are linked to radial graben. This relation suggests that dikes were emplaced in the subsurface. Embayment of the annulus of ridges on the NNW and a rim of horsts and graben on the N and NNE of Quetzalpetlatl (Fig. 19, A and C), infilling of the peripheral moat on the NW, and burial of NW-trending radial fractures in the corona interior demonstrate that pervasive volcanism occurred after these tectonic structures were formed. The background radar-dark plains contain graben oriented both parallel (oldest) and normal (youngest) to the moat. The earliest flows that flood the moat (a unit of intermediate brightness) embay both graben sets. The two later radar-bright flows have digitate lobes along the strike of the graben; these relations suggest that faulting was still active subsequent to the emplacement of the first flows. Few fractures cut the latest unit.

In summary, volcanism was concentrated on the large caldera-like structure in the southeast part of the corona. Volcanism was apparently linked to the uplift and radial fracturing, and was largely superposed on the fractures. Subsequent to the formation of the deformed annulus, volcanism continued in both the corona interior and exterior. The most recent volcanism appears to be concentrated in the caldera region.

A quasi-circular corona-like structure 130 km in overall diameter (59°S, 350°) located 1250 km NW of Quetzalpetlatl and 65 km west of the source of Mylitta Fluctus (Fig. 18), is also characterized by complex faulting and volcanism (Fig. 20). To the SE and east are several small radar-bright units and numerous small volcanic domes [see figure 22 in (*57*)]. This corona-like feature is a broad gentle dome rising about 1 km from the surrounding plains. Two well-developed zones of radar-dark lava flows originate near the summit and extend down the flank. The sources appear to be steep-walled pits or calderas near the inner margin of the semicircular annulus of fractures on the western side of the structure. The northern flow has been funneled through a structurally defined trough that runs down the flank of the dome [see figure 22B in (*57*)]. The lavas ponded as they emanated from this trough, and now obscure underlying structures.

The interior of the corona-like structure is generally smooth; it is characterized by a number of small volcanic features including chains of pits several kilometers across aligned both radially and concentrically. Also present in the center of the structure are volcanic mounds that are typically 1.5 to 4 km in diameter and generally contain small pits at their centers. They are morphologically similar to small volcanic edifices elsewhere on the planet. A 5-km-diameter depression near the center has a distinct raised rim. A long lava channel begins at about 58.5°S, 350° from a circular depression about 2.5 km across and proceeds NNE, cutting the northeast sector of the semicircular fractures. It eventually splits and terminates in diffuse flows. The diversity of volcanic features and the presence of numerous steep-sided domes and cones suggest that some viscous magmas may have been erupted, and possibly that the composition of magma changed with time. To the SE, three elongate depressions similar to troughs observed in the interior of Quetzalpetlatl are aligned with a NW-trending fracture system [see figure 19 in (*57*)].

Both the corona-like feature and the shield that is the source for Mylitta Fluctus lie along the same linear deformation zone (*59*). The absence of concentric and radial structures of the corona-like feature in the east suggests that the Mylitta source volcano formed after this radial fracturing. In addition, flows on the southern flank of the volcano turn eastward, as if responding to the positive topography of the corona-like feature. However, concentric graben in the north appear to cut the base of the volcano, and many of the volcanic features in the corona-like feature appear superposed on deposits of the Mylitta source volcano. These relations suggest that the two structures formed concurrently. The two similar-sized features thus illustrate contrasting styles associated with upwelling along a rift zone: the corona-like feature is dominated by structural deformation (concentric and radial fractures), and volcanism is of minor volumetric importance, whereas Mylitta Fluctus is dominated by volcanism.

Upland rises are broad topographic highs

Fig. 19. Quetzalpetlatl corona (68°S, 355°) in northern Lada Terra (*81*). (**A**) Magellan radar image of the rim and interior. Radial fractures dominate the eastern portion of the image, while the concentric annulus of deformed terrain is seen in the right center. Lava flows radiate from the interior (bottom), and multiple flow units have flooded the moat exterior to the deformed zone. Width of image in center is about 450 km. (**B**) Interior caldera showing the oval concentric fractures and multiple volcanoes, flows, and sinuous channels. Width of image is about 180 km. (**C**) Northwest edge of Quetzalpetlatl and surrounding region. Details of the lava flow stratigraphy in the moat are visible and the radial graben outside the corona are embayed by flow units. Width of image is about 275 km.

located primarily along the Equatorial Highlands and characterized by associated rifting and volcanism (*29*). Magellan data have revealed the characteristics of one of these rises (Western Eistla Regio), a broad highland region about 2000 km wide and 2800 km long (Fig. 5A). Sif and Gula Montes are situated on the rise and are linked to rift zones cutting NW-SE across the rise (*6, 32*) (Fig. 5). At least three smaller shields or volcanic centers are also located on the rise, amid patches of tessera terrain. The volcanism and setting in Western Eistla Regio differs from the linear deformation zone of northern Lada Terra in that Eistla: (i) is less linear and more complex; (ii) is broader, and contains more volcanoes that are more broadly distributed on the rise; and (iii) contains tessera terrain. Western Eistla Regio may be more similar to tectonic junctions such as Beta Regio (*65*). The broad distribution of volcanism in Western Eistla is suggestive of a wide region of melting in the subsurface. Whether this represents differences in the planform or scale of convection from that beneath linear deformation zones or different stages in the evolution of mantle upwelling is not known.

Linear zones of crustal shortening occur in at least two environments on Venus, mountain belts and ridge belts. Major questions in the understanding of the mountain belts are their thermal structure and whether the thickened crust has melted. Magellan data reveal the detailed characteristics of some of the mountain belts in Western Ishtar Terra (*57*). In the eastern part of Freyja Montes there is little evidence for volcanism even in areas that appear to be undergoing extension and gravitational relaxation. Volcanism is common, however, in the outboard plateau to the north (Itzpapalotl Tessera). Here, linear belts parallel to Freyja are locally covered by zones of smooth plains (*66*) of volcanic deposits (Fig. 21). In some cases, plains appear to be related to sinuous channels hundreds of kilometers long with sources in the adjacent high parts of the tessera (Fig. 21). In addition, Magellan data confirm that plains seen in the outboard foredeep at the base of Uorsar Rupes have a volcanic origin (*7, 36, 66*). Here, flows have embayed the base of the scarp and filled in the foredeep (Fig. 21). The location of volcanic activity suggests that the thermal gradients in the thickened crust of the mountains are less than near the edge of the plateau and that material underthrust at the edge may be undergoing melting. The lack of distinctive edifices and the apparently fluid nature of the lavas (Fig. 21) are consistent with predictions that iron-rich basalts should be the product of underthrusting and melting of anhydrous basaltic crust on Venus (*16*). Inboard of Freyja Montes, volcanic deposits on the plains in Lakshmi Planum are involved in the deformation of Freyja (*37*), but their sources appear to be linked to central Lakshmi (*37*), not to the mountain belt.

In contrast, crater chains, troughs, and associated sinuous structures are abundant in Danu Montes (Fig. 22). Volcanism is apparently linked to extensional deformation (graben oriented NW-SE) associated with gravitational relaxation of the mountain range (*57*). Some of the sources are linked to plains deposits at the base of the mountains both on the outboard (Vesta Rupes) and inboard (Lakshmi Planum) sides [see figures 11 and 12 in (*57*)]. In addition, volcanic plains occur in the outboard foredeep south of Danu Montes (*67*). Danu Montes, with its lower topography and more abundant evidence of extensional deformation than Freyja Montes, may be relatively older than Freyja Montes, and thus sufficient time may have elapsed for heating of the thickened crust.

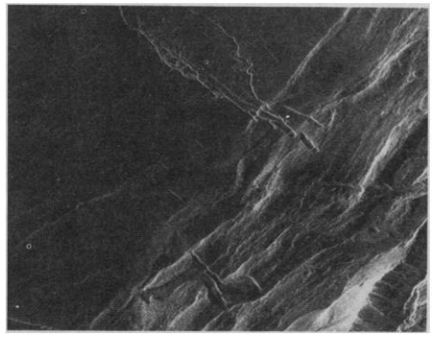

Fig. 22. Crater chains, volcanic plains, and flooded graben in northeast Danu Montes.

Ridge belts have also been interpreted to be of compressional origin (*5, 68, 69*), although extensional origins have been proposed (*70*). Magellan data reveal that the ridge belts in Lavinia Planitia are characterized by a complex combination of features interpreted to represent compression, shear, and extension (*57*). Volcanism, in the form of plains and associated small shields, is superposed on several deformed belts, as shown by the embayment relations of deposits from Mylitta Fluctus (Fig. 18, A and B) and other volcanic centers (*57–59*). These relations suggest that subsurface melting is occurring in these deformed zones. Whether this is linked to crustal thickening and shortening (*57*) or is simply related to local mantle upwelling is not known, although the generally low topography of the region would not favor the latter explanation.

Only one example of a highland plateau is known to date on Venus. Situated in Western Ishtar Terra and surrounded by orogenic belts (*71*), Lakshmi Planum is elevated about 3 to 4 km above the mean planetary radius and consists of volcanic plains and two large volcanic centers (Colette and

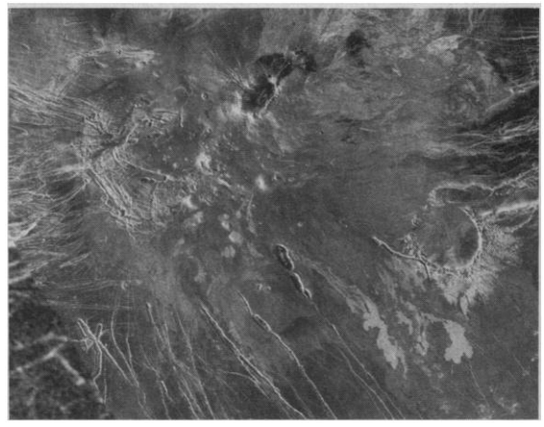

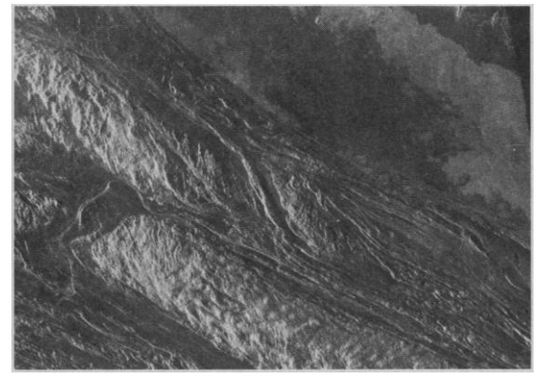

Fig. 20 (**left**). Corona-like feature about 130 km in overall diameter in northern Lada Terra (59°S, 350°) about 1250 km northwest of Quetzalpetlatl corona. This structure is just SW of the edifice associated with Mylitta Fluctus (Fig. 18D). A wide variety of volcanological features are seen in the center and SE flanks of this structure.

Fig. 21 (**right**). Volcanic plains in northern Itzpapalotl Tessera north of Freyja Montes. A sinuous rille about 2 km wide begins in the narrow zone parallel to the mountains and is linked to the emplacement of radar-dark plains in low areas between the mountains. The distinctive break between the SW and NE parts of the image is Uorsar Rupes, a scarp marking a several-kilometer topographic drop. The outboard foredeep to the north contains additional radar-bright and -dark volcanic plains.

Sacajawea). The origin and significance of Lakshmi Planum has been controversial, and ideas have ranged from a hot-spot origin (upwelling and outflow of mantle material to produce the mountain ranges) (*36*), to underthrusting of crust beneath a tessera block and subsequent melting and volcanism (*72*). Understanding the origin of Sacajawea (Fig. 7) and its relations with adjacent terrain is thus important. Magellan data indicating the presence of a neutral buoyancy zone at depth below Sacajawea (*37, 38, 73*) were described above. In addition, evidence for radial fractures and uplift adjacent to Sacajawea (grooved plains) observed in Venera 15–16 data (*36, 37*) has been confirmed, as has the presence of tessera (*36, 37*). Some tessera directly north of Sacajawea appears to be composed of crosscutting graben in volcanic plains; thus at least the latest formation of tessera may be coincident with the formation of the plains.

Impact craters observed thus far (*74*) are largely unmodified by volcanism in their exteriors, with the marked exception of the crater south of Myllitta Fluctus (Fig. 18D) which has been breached and flooded. A number of craters show evidence for smooth plains in their interiors, and although these may be impact melt deposits, the possibility of volcanic flooding or impact-triggered volcanism should be considered.

Tesserae are highly deformed upland regions comprising about 15% of the terrain surveyed by Venera 15–16 (*7, 58, 59, 75, 76*). The tessera at Alpha Regio show numerous small shield volcanoes within patches of dark smooth plains embaying adjacent structures (Fig. 23). These volcanic plains probably originate from the shield volcanoes. The patches are widely distributed in area, elevation, and size. In some cases, plains have been subsequently cut by graben; thus emplacement of volcanic deposits may have been contemporaneous with at least the latter parts of the deformation. The patchy distribution and lack of large edifices and centers of volcanism in Alpha suggest that volcanism is relatively local.

Synthesis. Volcanic plains and edifices make up more than 80% of the surface observed thus far, as noted in lower-resolution data of the same area covered by Venera 15–16 (7) and Arecibo (*6, 59*). The rest of the surface, generally occupied by tectonically deformed regions (*57*), is likely to be deformed volcanic deposits.

Insufficient data are available to assess the mode of formation of the crust. Although localized sources of volcanic activity clearly contribute to the crust by resurfacing, we do not know whether the crust forms and evolves predominantly by uniform vertical thickening, serial emplacement, or by lateral

Fig. 23. Patches of volcanic plains in Alpha Regio (24.6°S, 3.8°). Radar-dark plains embay the tessera, and small shield volcanoes less than about 5 km across are seen.

accretion (*56, 17, 77*). Global coverage of volcanic and tectonic structures and units and improved estimates of surface ages will permit more complete assessment of crustal formation processes and rates. Also not known is whether the crust is predominantly basaltic in nature [the secondary crust of Taylor (*78*)] or whether tertiary crust (derived from reworked or evolved secondary crust) is volumetrically important (*14*). This question remains open because of the likelihood of compositional diversity in different environments (*16*), the Venera 8 data (*12, 13*), and the discovery of domes analogous to rhyolite-dacite domes on Earth (Fig. 9).

The coronae observed thus far, characterized by complex and diverse central volcanism and abundant effusive volcanism, may be linked to hot spots. If these hot spots are like those on Earth, then picritic melts are likely to be produced from the hot central core and tholeiitic melts from the cooler plume margins. If Venus plumes are 100° to 150°C hotter than their terrestrial counterparts, melts in the central core will resemble basaltic komatiites, and those in the margins would be MgO-rich tholeiites (*16*). Volcanic centers on linear deformation zones of extensional origin (rift-like features), characterized by corona-like upwellings (Fig. 20) and shield volcanoes (Mylitta Fluctus; Fig. 18), are likely linked to extension and pressure-release melting (*79*). Volcanism associated with upland rises such as Western Eistla Regio is related to apparent broad uplifts and rift-like zones, and apparently linked to large-scale mantle upwelling. Ridge belts in Lavinia Planitia form by the deformation of volcanic plains and are also the site of local patches of plains and small shields superposed on the deformed belts. Some mountain belts, such as Danu Montes, show signs of volcanism associated with extension and gravitational relaxation, whereas Freyja Montes, perhaps younger, has volcanism only in the outboard flanking regions where active underthrusting may be occurring. Volcanism associated with tessera appears to be patchy, localized, and volumetrically small. If the highland plateau of Lakshmi Planum is a tessera block, it is unlike other tessera in the volume of volcanic deposits and the presence of large calderas (Colette and Sacajawea). This difference may be related to its location surrounded by mountain belts or to the presence of subjacent hot spots.

On the basis of impact crater density, the age of the surface of Venus is relatively young (average age <1 Ga) (*74*). The Sappho and southern Lavinia regions have few such craters and are thus the sites of the most recent regional volcanological activity (*74*). These new data do not change earlier estimates of the rates of global volcanic resurfacing [less than 2 km^3/yr (*80*)].

There are many outstanding questions (*77*). A wide diversity of melts is possible in different petrogenetic environments on Venus. Mantle melts could include such diverse products as quartz tholeiites, komatiites, and kimberlites; remelted crust could include ferrobasalts, andesites, and dacites (*16*). An important challenge is to develop criteria to identify the morphologic characteristics and environments of such diverse deposits. The significance of dike formation and intrusions (as suggested by the abundant fractures and graben) and implications for the ratio of intrusion to extrusion, remain to be established. The range of modes of crustal formation and loss, their relative significance, and their rates, are incompletely known. Acquisition of a global data set by Magellan will provide data to address these questions.

REFERENCES AND NOTES

1. R. S. Saunders and M. C. Malin, *Geophys. Res. Lett.* **4**, 547 (1977).
2. G. H. Pettengill *et al.*, *J. Geophys. Res.* **85**, 8261 (1980).
3. H. Masursky *et al.*, *ibid.*, p. 8232.
4. BVSP (Basaltic Volcanism Study Project), *Basaltic Volcanism on the Terrestrial Planets* (Pergamon, New York, 1981).
5. V. L. Barsukov *et al.*, *J. Geophys. Res.* **91**, 378 (1986).
6. D. B. Campbell *et al.*, *Science* **246**, 373 (1989).
7. A. L. Sukhanov *et al.*, *U.S. Geol. Surv. Misc. Invest. Ser. Map I-2059* (1989).
8. J. C. Aubele and E. N. Slyuta, *Earth Moon Planets* **50/51**, 493 (1990).
9. G. G. Schaber, *Proc. 21st Lunar Planet. Sci. Conf.*, in press.
10. Yu. A. Surkov, V. L. Barsukov, L. P. Moskalyeva, V. P. Kharyukova, A. L. Kemurdzhian, *Proc. 14th Lunar Planet. Sci. Conf.*, *J. Geophys. Res.* **89**, B393 (1984).
11. Yu. A. Surkov *et al.*, *Proc. 17th Lunar Planet. Sci. Conf.*, *J. Geophys. Res.* **92**, E537 (1987).

12. Yu. A. Surkov *et al.*, *Kos. Issled.* **14**, 704 (1976).
13. Yu. A. Surkov *et al.*, *Proc. Lunar Sci. Conf.* **8**, 2665 (1977).
14. O. V. Nikolaeva, *Earth Moon Planets* **50/51**, 329 (1990).
15. J. W. Head and L. Wilson, *J. Geophys. Res.* **91**, 3049 (1986).
16. P. C. Hess and J. W. Head, *Earth Moon Planets* **50/51**, 57 (1990).
17. C. Sotin, D. A. Senske, J. W. Head, E. M. Parmentier, *Earth Planet. Sci. Lett.* **95**, 321 (1989).
18. D. R. Williams and V. Pan, *Geophys. Res. Lett.* **17**, 1397 (1990).
19. G. H. Pettengill *et al.*, *Science* **252, 260** (1991).
20. G. L. Tyler *et al.*, *ibid.*, p. 265.
21. E. N. Slyuta *et al.*, *Astron. Vestn.* **22**, 287 (1988).
22. J. B. Garvin and R. S. Williams, *Geophys. Res. Lett.* **17**, 1381 (1990).
23. D. L. Swanson *et al.*, *U.S. Geol. Surv. Prof. Pap.* **1056**, 1 (1979).
24. R. Greeley, *J. Geophys. Res.* **87**, 2705 (1982).
25. M. H. Carr, *Icarus* **22**, 1 (1974); G. Hulme, *Mod. Geol.* **4**, 107 (1973).
26. J. W. Head and L. Wilson, *Lunar Planet. Sci.* **XI**, 426 (1980).
27. R. Greeley, *Science* **172**, 722 (1971).
28. E. N. Slyuta and M. A. Kreslavsky, *Lunar Planet. Sci.* **XXI**, 1174 (1990).
29. D. A. Senske, *Earth Moon Planets* **50/51**, 305 (1990).
30. E. N. Slyuta, *Lunar Planet. Sci.* **XXI**, 1172 (1990).
31. G. G. Schaber and R. C. Kozak, *U.S. Geol. Surv. Open File Rep.* **90-24** (1990).
32. D. A. Senske *et al.*, *Earth Moon Planets*, in press.
33. B. A. Campbell and D. B. Campbell, *Geophys. Res. Lett.* **17**, 1353 (1990).
34. L. Wilson, J. W. Head, and D. B. Campbell, *Lunar Planet. Sci.* **XXI**, 1347 (1990).
35. H. Sigurdsson and R. S. J. Sparks, *Nature* **274**, 126 (1978).
36. A. A. Pronin, *Geotectonics* **20**, 271 (1986).
37. K. M. Roberts and J. W. Head, *Earth Moon Planets* **50/51**, 193 (1990).
38. L. Wilson and J. W. Head, *Lunar Planet. Sci.* **XXI**, 1343 (1990).
39. C. Elachi *et al.*, *IEEE Trans. Geosci. Rem. Sens.* **GE22**, 383 (1984).
40. J. E. Guest and J. Sanchez, *Bull. Volcanol.* **33**, 778 (1969); B. Bonnichsen and D. F. Kaufman, *Geol. Soc. Am. Spec. Pap.* **212**, 119 (1987).
41. J. H. Fink and Manley (1987) *Geol. Soc. Am. Spec. Pap.* **212**, 77 (1987).
42. D. L. Swanson and R. T. Holcomb, in *Lava Flows and Domes*, J. H. Fink, Ed. (Springer-Verlag, Berlin, 1990), pp. 3–24.
43. R. M. Iverson, in *ibid.*, pp. 47–69.
44. S. Blake, in *ibid.*, pp. 88–126.
45. J. H. Fink, M. C. Malin, S. W. Anderson, *Nature* **348**, 435 (1990).
46. H. Williams, *Bull. Dept. Geol. Sci. Univ. Calif.* **21**, 51 (1932).
47. J. H. Fink, Ed. *Geol. Soc. Am. Spec. Pap.* **212** (1987).
47a. A. T. Basilevsky, personal communication.
48. J. A. Crisp, *J. Volcanol. Geotherm. Res.* **20**, 177 (1984).
49. A. Knopf, *Geol. Soc. Am. Bull.* **47**, 1727 (1936).
50. K. Nakamura, *J. Volcanol. Geotherm. Res.* **2**, 1 (1977).
51. G. G. Schaber, C. Elachi, T. G. Farr, *Remote Sens. Environ.* **9**, 149 (1980).
52. J. A. Crisp and S. Baloga, *Icarus* **85**, 512 (1990).
53. L. Wilson and J. W. Head, *Lunar Planet. Sci.* **XI**, 1260 (1980).
54. H. Huppert *et al.*, *Nature* **309**, 19 (1984).
55. R. S. Saunders *et al.*, *Science* **252, 249** (1991).
56. J. W. Head, *Earth Moon Planets* **50/51**, 5 (1990).
57. S. C. Solomon *et al.*, *Science* **252**, 297 (1991).
58. D. B. Campbell *et al.*, *ibid.* **251**, 181 (1991).
59. D. A. Senske *et al.*, *Earth Moon Planets*, in press.
60. V. P. Kryuchkov and A. T. Basilevsky, *Lunar Planet. Sci.* **XX**, 548 (1989).
61. T. L. Tolan *et al.*, *Geol. Soc. Am. Spec. Pap.* **239**, 1 (1989).
62. V. L. Barsukov *et al.*, *Geochimica* **12**, 1811 (1984).
63. E. R. Stofan and J. W. Head, *Icarus* **83**, 216 (1990).
64. A. A. Pronin and E. R. Stofan, *ibid.* **87**, 452 (1990).
65. D. A. Senske *et al.*, *Lunar Planet. Sci.* **XXI**, 1128 (1990).
66. J. W. Head, *Geology* **18**, 99 (1990).
67. _____ and J. D. Burt, *Lunar Planet. Sci.* **XXI**, 481 (1990).
68. V. P. Kryuchkov, *Earth Moon Planets* **50/51**, 471 (1990).
69. S. L. Frank and J. W. Head, *ibid.*, p. 421.
70. A. L. Sukhanov and A. A. Pronin, *Proc. Lunar Planet. Sci. Conf.* **19**, 335 (1989).
71. L. S. Crumpler *et al.*, *Geology* **14**, 1031 (1986).
72. K. M. Roberts and J. W. Head, *Geophys. Res. Lett.* **17**, 1341 (1990).
73. L. Wilson, J. W. Head, E. A. Parfitt, *Vernadsky/Brown Microsymp. 12* **2**, 37 (1990).
74. R. J. Phillips *et al.*, *Science* **252, 288** (1991).
75. A. L. Sukhanov *et al.*, *Astron. Vestn.* **21**, 195 (1987).
76. D. L. Bindschadler and J. W. Head, *J. Geophys. Res.*, in press.
77. S. C. Solomon and J. W. Head, *Science* **252**, 252 (1991).
78. S. R. Taylor, *Tectonophysics* **161**, 147 (1989).
79. R. White and D. McKenzie, *J. Geophys. Res.* **94**, 7685 (1989).
80. R. E. Grimm and S. C. Solomon, *Geophys. Res. Lett.* **14**, 538 (1987).
81. Quetzalpetlatl Corona and Mylitta Fluctus have been proposed as names to the IAU, but as of this writing the names have not been officially approved.
82. Unpublished maps by A. T. Basilversky (personal communication) aided our interpretation.
83. We gratefully acknowledge the Magellan Team at JPL, Martin-Marietta, and Hughes for their dedication to obtaining the data. D. Senske prepared the maps of Sif Mons and contributed to the discussion of Western Eistla Regio. K. Roberts prepared the maps of Sacajawea Patera and contributed to the discussion of Sacajawea and Mylitta Fluctus. J. Aubele and E. Slyuta prepared maps of the small shields and contributed to the discussion. B. Klose and B. Pavri contributed to the discussion of the steep-sided domes. D. Bindschadler and E. Stofan contributed to the discussion of the coronae. S. Keddie contributed to the discussion of cryptodomes. P. Fisher, E. Grosfils, A. deCharon, M. Bulmer, A. T. Basilevsky, V. Kryuchkov, and T. Parker contributed to the discussion and review of this paper. Special thanks to S. Yewell, J. Clark, J. Clough, and R. Post for preparation of images and figures. We gratefully acknowledge helpful reviews from J. Garvin and an anonymous reviewer.

22 January 1991; accepted 20 March 1991

Impact Craters on Venus: Initial Analysis from Magellan

ROGER J. PHILLIPS, RAYMOND E. ARVIDSON, JOSEPH M. BOYCE, DONALD B. CAMPBELL, JOHN E. GUEST, GERALD G. SCHABER, LAURENCE A. SODERBLOM

Magellan radar images of 15 percent of the planet show 135 craters of probable impact origin. Craters more than 15 km across tend to contain central peaks, multiple central peaks, and peak rings. Many craters smaller than 15 km exhibit multiple floors or appear in clusters; these phenomena are attributed to atmospheric breakup of incoming meteoroids. Additionally, the atmosphere appears to have prevented the formation of primary impact craters smaller than about 3 km and produced a deficiency in the number of craters smaller than about 25 km across. Ejecta is found at greater distances than that predicted by simple ballistic emplacement, and the distal ends of some ejecta deposits are lobate. These characteristics may represent surface flows of material initially entrained in the atmosphere. Many craters are surrounded by zones of low radar albedo whose origin may have been deformation of the surface by the shock or pressure wave associated with the incoming meteoroid. Craters are absent from several large areas such as a 5 million square kilometer region around Sappho Patera, where the most likely explanation for the dearth of craters is volcanic resurfacing. There is apparently a spectrum of surface ages on Venus ranging approximately from 0 to 800 million years, and therefore Venus must be a geologically active planet.

IMPACT CRATERS ON VENUS PROVIDE new information on the physics of cratering processes, including interaction with the atmosphere during meteoroid transit and atmospheric effects on cratering mechanics and ejecta formation. The modification of impact craters yields information on surface and interior processes, particularly tectonism and volcanism. The geographical distribution and abundance of craters provide constraints on the rate of resurfacing of the planet and, thus, the level of geological activity over the last several hundred million years.

After 37 days of operation, or 277 orbits covering approximately 56° of longitude, a total of 135 craters ranging from 3 to 105 km in diameter have been interpreted as having a high probability of impact origin. They lie within an area of 70×10^6 km^2, or about 15% of the planet's surface. If the area

R. J. Phillips, Department of Geological Sciences, Southern Methodist University, Dallas, TX 75275.
R. E. Arvidson, McDonnell Center for the Space Sciences, Department of Earth and Planetary Sciences, Washington University, St. Louis, MO 63130.
J. M. Boyce, Solar System Exploration Division, National Aeronautics and Space Administration, Washington, DC 20546.
D. B. Campbell, Department of Astronomy, Cornell University, Ithaca, NY 14853.
J. E. Guest, University of London Observatory, London, NW7 2QS England.
G. G. Schaber and L. A. Soderblom, U.S. Geological Survey, Flagstaff, AZ 86001.